A General Acid−Base Mechanism for the Stabilization of a Tetrahedral Adduct in a Serine−Carboxyl Peptidase: A Computational Study

Haobo Guo,[†] Alexander Wlodawer,[‡] and Hong Guo*,[†]

Department of Biochemistry and Cellular and Molecular Biology and Center of Excellence for Structural Biology, University of Tennessee, Knoxville, Tennessee 37996, and Protein Structure Section, Macromolecular Crystallography Laboratory, National Cancer Institute at Frederick, Frederick, Maryland 21702

Received March 31, 2005; E-mail: hguo1@utk.edu

Sedolisins (serine−carboxyl peptidases) belong to a recently characterized family of proteolytic enzymes (MEROPS S53) that have a fold resembling that of subtilisin and a maximal activity at low pH.[1] This family includes the peptidase CLN2,[2] a human enzyme for which mutations in the encoding *CLN2* gene lead to a fatal neurodegenerative disease, classical late-infantile neuronal ceroid lipofuscinosis.[3] The defining features of the sedolisin family are a unique catalytic triad,[4,5] Ser-Glu-Asp (Ser278-Glu78-Asp82 for kumamolisin-As; see Figure 1), as well as the presence of an aspartic acid residue (Asp164 for kumamolisin-As) that replaces Asn155 of subtilisin, a residue that creates the oxyanion hole. The X-ray crystallographic and mutagenesis studies[4,5] demonstrated that the serine residue is the catalytic nucleophile, while the nearby Glu is likely to act as the general base to accept the proton from Ser and assist in the nucleophilic attack. A fundamental question for serine−carboxyl peptidases is whether these enzymes use the catalytic mechanism similar to that of classical serine proteases with simple replacements of certain catalytic residues so that they could be active at low pH. Here we demonstrate from quantum mechanical/molecular mechanical (QM/MM) molecular dynamics (MD) simulations that this may not be the case. Unlike serine proteases that use the oxyanion−hole interactions to achieve the electrostatic stabilization of the tetrahedral intermediate and adduct, the members of the sedolisin family seem to stabilize the tetrahedral intermediate and adduct primarily through a general acid−base mechanism (i.e., similar to the mechanism proposed for aspartic proteases[6]).

In this Communication, the QM(SCC-DFTB)/MM MD and free energy simulations[7] have been performed on kumamolisin-As. We examined the role of the active site residues in the stabilization of a tetrahedral adduct (hemiacetal) by an inhibitor *N*-acetyl-isoleucyl-prolyl-phenylanial (AcIPF) and elucidated the mechanistic similarities and differences between serine proteases and a member of the sedolisin family. The average structure of the active site for the tetrahedral adduct complex obtained from the simulations is given in Figure 1. As is evident from Figure 1, the structure obtained from the simulations is very close to the experimental structure. For the aldehyde complex, two average structures are shown in Figure 2A and B, respectively. Both structures were found to be well populated from the simulations, suggesting that their stabilities do not differ significantly. As illustrated in Figure 2A, a low-barrier hydrogen bond was formed in the substrate analogue complex. This is in contrast to the case of serine proteases, where low-barrier hydrogen bonds were found in transition state analogue complexes.[15] It has been a subject of debate as to whether the low-barrier hydrogen bonds in serine proteases might play an important role in transition state stabilization.[15] For kumamolisin-As, a large stabilizing effect for the aldehyde complex was not observed as a result of the low-barrier hydrogen bond formation.
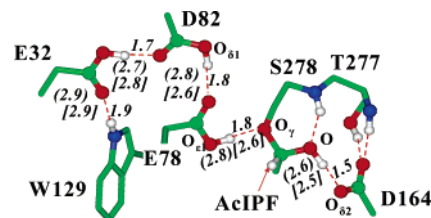
Figure 1. The average active site structure of the kumamolisin-As−tetrahedral adduct complex. The hydrogen bond distances (in Å) between the non-hydrogen atoms are also given (in parentheses) and compared with those from the X-ray structure (in square brackets).[4a]
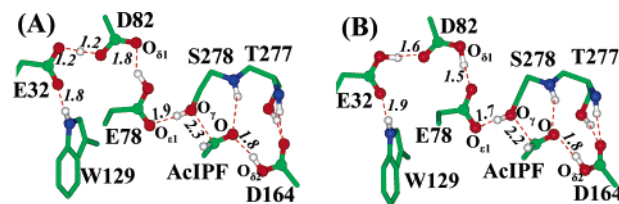

Figure 2. (A, B) Two average structures of the aldehyde complex.

Comparison of the structures in Figure 1 and Figure 2A,B shows that the proton on $O_{\epsilon 1}$ of Glu78 (O_γ of Ser278) transfers to O_γ of Ser278 ($O_\epsilon 1$ of Glu78) as the hemiacetal (aldehyde) changes to the aldehyde (hemiacetal), supporting the earlier suggestion[4,5] that Glu78 plays a role similar to that of His57 in subtilisin. In the initial model of the hemiacetal complex, the proton between $O_{\delta 2}$ of Asp164 and O of the hemiacetal was assumed to be on $O_{\delta 2}$. This proton moved to O after energy minimization and MD simulations; the same proton transfer was also observed with a high level QM-(B3LYP)/MM minimization. We have tried to fix this proton on Asp164 by using the MM treatment of the protonated Asp164, and this led to the breakdown of the hemiacetal complex. Thus, the results indicate that Asp164 is deprotonated in the hemiacetal complex, and this suggestion is supported by free energy simulations (see below).

The change of free energy (potential of mean force) as a function of the reaction coordinate (ξ) for the interconversion between the hemiacetal and aldehyde complexes is given in Figure 3A for the wild-type enzyme and mutants Asp164Asn and Thr277Ala. Figure 3B shows the average structures for the wild-type enzyme at points a, b, and c along the reaction coordinate (ξ). Although both structures of Figure 2A and B were observed for the aldehyde complex, the nucleophilic attack actually starts from the structure with the unprotonated Glu78 (i.e., through the one proton-transfer mechanism). For serine proteases, the question as to whether the catalytic triad uses one proton transfer or two proton-transfer mechanisms has been a subject of debate.[15b] The results on kumamolisin-As indicate that the structures for the stable complexes may not be sufficient to identify the correct mechanism for the reaction.
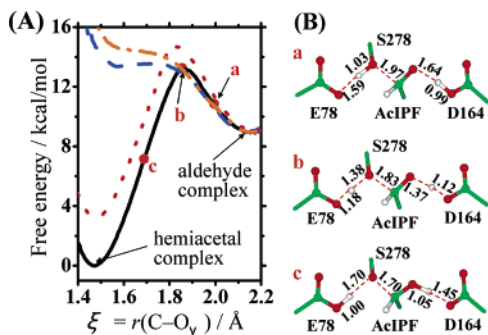
Figure 3. (A) The free energy change between the hemiacetal and aldehyde complexes as a function of $\xi = r(C-O_\gamma)$ for wild-type (with and without the QM treatment of Asp164), Asp164Asn, and Thr277Ala. Black solid line: wild-type. Blue dashed line: wild-type with Asp164 treated by MM. Orange dot–dashed line: Asp164Asn. Red dot line: Thr277Ala. (B) The average structures of the active site of the wild-type enzyme along the reaction coordinate at points a, b, and c shown in Figure 3A.

Figure 3A shows that for the wild-type enzyme the hemiacetal complex is significantly more stable than the aldehyde complex. One important event during the interconversion between the hemiacetal and aldehyde complexes is the proton transfer between Asp164 and the ligand (see Figure 3B). To see if this proton transfer is important for the stability of the tetrahedral adduct, we used the MM treatment for protonated Asp164 and repeated the free energy simulations. The hemiacetal complex became considerably less stable than the aldehyde complex when the proton transfer from Asp164 to the ligand was prevented by the MM treatment. To further examine the importance of this proton transfer, the free energy simulations for Asp164Asn were performed. Figure 3A shows that the replacement of Asp164 by asparagine destabilizes the hemiacetal complex considerably, providing additional support for the general acid–base mechanism in stabilizing the tetrahedral adduct. There is a decrease of the relative stability of the hemiacetal in Thr277Ala, indicating that the hydrogen bond from Thr277 may stabilize the hemiacetal through the stabilization of the charge formation on Asp164.

The results of the simulations show that the members of sedolisin family may evoke different catalytic machineries than classical serine proteases in achieving transition state stabilization. Unlike serine proteases that use the oxyanion–hole interactions to achieve the electrostatic stabilization of the tetrahedral intermediates and adducts, these enzymes seem to stabilize the tetrahedral intermediates and adducts primarily through a general acid–base mechanism. Consistent with this suggestion, the Asp164Ala mutant of kumamolisin did not show any measurable proteolytic activity.[5a] It should be pointed out that our conclusion is based on the large free energy difference for the two different mechanisms and that care must be exercised in using the free energy profiles for quantitative discussions. For yeast chorismate mutase, for which a protonated carboxyl group from Glu246 is involved in the electrostatic stabilization of the transition state rather than a general acid–base catalysis,[16] replacement of Glu246 by glutamine does not lead to a reduction of k_{cat}/K_M but rather changes the pH optimum for the activity from a narrow to a broad pH range. The results reported here suggest that this is unlikely to be the case for sedolisins, and that there may be a significant loss of the activity due to the Asp164→Asn mutation. Consistent with this suggestion, for aorsin (a member of the sedolisin family), replacement of Asp164 (kumamolisin-As numbering) by asparagine leads to a reduction in k_{cat}/K_M by a factor of 1×10^{-4}.[17] This reduction of the activity is comparable to that of replacement of Glu78 (kumamolisin-As numbering) by glutamine; the same observation was made for human tripeptidyl-peptidase (CLN2 protein).[2c] For aspartic proteases, it has been proposed that

conformational changes/fluctuations may play a role in the catalysis.[6c–d] This could be the case for sedolisins, as well. For instance, comparison of the structures of kumamolisin and the Ser278Ala mutant of pro-kumamolisin[5] indicates that the breaking of the salt bridge(s) of Asp164 with nearby positively charged residues (e.g., the P3-Arg residue of the prepeptide) in pro-kumamolisin during secretion into acidic medium might trigger conformational changes and generate the well-positioned general-acid catalyst Asp164, leading to the self-activation.

Supporting Information Available: A description of the computational methods used in the present study, additional structures obtained from the simulations, and complete ref 10. This material is available free of charge via the Internet at http://pubs.acs.org.

References

(1) (a) Wlodawer, A.; Li, M.; Gustchina, A.; Oyama, H.; Dunn, B. M.; Oda, K. *Acta Biochim. Pol.* **2003**, *50*, 81−102. (b) Vandeputte-Rutten, L.; Gros, P. *Curr. Opin. Struct. Biol.* **2002**, *12*, 704−708. (c) Powers, J. C.; Asgian, J. L.; Ekici, O. D.; James, K. E. *Chem.* Rev. **2002**, *102*, 4639−4750. (d) Wlodawer, A. *Structure* **2004**, *12*, 1117−1119.

(2) (a) Rawlings, N. D.; Barrett, A. J. *Biochim. Biophys. Acta* **1999**, *1429*, 496−500. (b) Linj, L.; Sohar, I.; Lackland, H.; Lobel, P. *J. Biol. Chem.* **2001**, *276*, 2249−2255. (c) Walus, M.; Kida, E.; Wisniewski, K. E.; Golabek, A. A. *FEBS Lett.* **2005**, *579*, 1383−1388.

(3) Sleat, D. E.; Donnelly, R. J.; Lackland, H.; Liu, C. G.; Sohar, I.; Pullarkat, R. K.; Lobel, P. *Science* **1997**, *277*, 1802−1805.

(4) (a) Wlodawer, A.; Li, M.; Gustchina, A.; Tsuruoka, N.; Ashida, M.; Minakata, H.; Oyama, H.; Oda, K.; Nishino, T.; Nakayama, T. *J. Biol. Chem.* **2004**, *279*, 21500−21510. (b) Wlodawer, A.; Li, M.; Dauter, Z.; Gustchina, A.; Uchida, K.; Oyama, H.; Dunn, B. M.; Oda, K. *Nat. Struct. Biol.* **2001**, *8*, 442−446. (c) Wlodawer, A.; Li, M.; Gustchina, A.; Dauter, Z.; Uchida, K.; Oyama, H.; Goldfarb, N. E.; Dunn, B. M.; Oda, K. *Biochemistry* **2001**, *40*, 15602−15611.

(5) (a) Comellas-Bigler, M.; Fuentes-Prior, P.; Maskos, K.; Huber, R.; Oyama, H.; Uchida, K.; Dunn, B. M.; Oda, K.; Bode, W. *Structure* **2002**, *10*, 865−876. (b) Comellas-Bigler, M.; Maskos, K.; Huber, R.; Oyama, H.; Oda, K.; Bode, W. *Structure* **2004**, *12*, 1313−1323.

(6) (a) Dunn, B. M. *Chem. Rev.* **2002**, *102*, 4431−4458. (b) Andreeva, N. S.; Rumsh, L. D. *Protein Sci.* **2001**, *10*, 2439−2450. (c) Cascella, M.; Micheletti, C.; Rothlisberger, U.; Carloni, P. *J. Am. Chem. Soc.* **2005**, *127*, 3734−3742. (d) Perryman, A. L.; Lin, J. H.; McCammon, J. A. *Protein Sci.* **2004**, *13*, 1108−1123.

(7) A semiempirical density-functional approach (SCC-DFTB)[8] recently implemented in the CHARMM program[9] was used for QM/MM MD and free energy simulations. The initial coordinates were obtained from the crystal structure (PDB ID: 1SIO) of kumamolisin-As, which has AcIPF covalently bound to Ser278.[4a] AcIPF and the side chains of Glu32, Asp82, Glu78, Ser278, and Asp164 were treated by QM and the rest of the system by MM. The all-hydrogen potential function (PARAM22)[10] was used for MM atoms. A modified TIP3P water model[11] was employed for the solvent. The stochastic boundary MD method[12] was used for the simulations. A 1 fs time step was used for integration of the equations of motion. The umbrella sampling method[13] along with the Weighted Histogram Analysis Method[14] was applied to determine the changes of the free energy.

(8) Cui, Q.; Elstmer, M.; Kaxiras, E.; Frauenheim, T.; Karplus, M. *J. Phys. Chem. B* **2001**, *105*, 569−585.

(9) Brooks, B., R.; Bruccoleri, R. E.; Olafson, B. D.; States, D. J.; Swaminathan, S.; Karplus, M. *J. Comput. Chem.* **1983**, *4*, 187−217.

(10) Mackerell, A. D., Jr. et al. *J. Phys. Chem. B* **1998**, *102*, 3586−3616.

(11) (a) Jorgensen, W. L. *J. Am. Chem. Soc.* **1981**, *103*, 335−340. (b) Neria, E.; Fisher, S.; Karplus, M. *J. Chem. Phys.* **1996**, *105*, 1902−1921.

(12) Brooks, C. L., III; Brunger, A.; Karplus, M. *Biopolymers* **1985**, *24*, 843.

(13) Torrie, G. M.; Valleau, J. P. *Chem. Phys. Lett.* **1974**, *28*, 578−581.

(14) Kumar, M.; Bouzida, D.; Swendsen, R. H.; Kollman, P. A.; Rosenberg, J. M. *J. Comput. Chem.* **1992**, *13*, 1011−1021.

(15) For reviews, see: (a) Frey, P. A. *J. Phys. Org. Chem.* **2004**, *17*, 511−520. (b) Hedstrom, L. *Chem. Rev.* **2002**, *102*, 4501−4523.

(16) Schnappauf, G.; Sträter, N.; Lipscomb, W. N.; Braus, G. H. *Proc. Natl. Acad. Sci. U.S.A.* **1997**, *94*, 8491−8496.

(17) Lee, B. R.; Furukawa, M.; Yamashita, K.; Kanasugi, Y.; Kawabata, C.; Hirano, K.; Ando, K.; Ichishima, E. *Biochem. J.* **2003**, *371*, 541−548.

JA0520565

A General Acid-Base Mechanism for the Stabilization of Tetrahedral Adduct in a Serine-Carboxyl Peptidase: a Computational Study

Haobo Guo[†], Alexander Wlodawer[‡], and Hong Guo*[,†]

[†]*Department of Biochemistry and Cellular and Molecular Biology, Center of Excellence in Structural Biology, University of Tennessee, Knoxville, Tennessee 37996-0840 and* [‡]*Protein Structure Section, Macromolecular Crystallography Laboratory, National Cancer Institute at Frederick, Frederick, MD 21702*

Contents:
- Computational methods;
- Additional structure figures: Figure S1~S3
- Complete Ref. 10

Computational Method

A fast semi-empirical density-functional approach (SCC-DFTB)[8] recently implemented in the CHARMM program[9] was used for quantum mechanical/molecular mechanical (QM/MM) molecular dynamics (MD) and free energy (potential of mean force or PMF) simulations. The initial coordinates for the simulations were obtained from the crystal structure (PDB ID:1SIO. Resolution: 1.80 Å) of kumamolisin-As complexed with the inhibitor AcIPF (*N*-acetyl-isoleucyl-prolyl-phenylanial) that is covelantly bound to Ser278.[4a]

The stochastic boundary molecular dynamics method[12] was used for QM(SCC-DFTB)/MM simulations. The system was separated into a reaction zone and a reservoir region; the reaction zone was further divided into the reaction region and buffer region. The reaction region was a sphere with radius R of 16 Å, and the buffer region had R equal to 16 Å $\leqslant$ R $\leqslant$ 18 Å. The reference center for partitioning the system was chosen to be the O_γ atom of Ser278 (see Figure 1A). The resulting system contains 3453 atoms (2700 enzyme atoms and 251 water molecules). The inhibitor AcIPF and the side chains of Glu32, Asp82, Glu78, Ser278 and Asp164 were treated by QM (a total of 92 QM atoms) and the rest of the system by MM. The all-hydrogen potential function (PARAM22)[5] was used for MM atoms. The link-atom approach (Reuter, N.; Dejaegere, A.; Maigret, B.; Karplus, M. *J. Phys. Chem. A* **2000**, *104*, 1720-1735) was used to separate the QM and MM regions. A modified TIP3P water model[11] was employed for the solvent. The initial structure for the entire stochastic boundary system was optimized by adopted basis Newton-Rhaphson (ABNR) method. The system was gradually heated from 50 to 310 K for 30 ps, and equilibrated at 310 K for 40 ps. A 1-fs time step was used for integration of the equations of motion, and coordinates were saved every 10 fs for analyses. The LD frictional constants were 250 ps^{-1} for the protein atoms and 62 ps^{-1} for the water molecules. The bonds involving hydrogen atoms in the MM region were fixed by the SHAKE algorithm (Ryckaert, J. P.; Ciccotti, G.; Berendsen, H. J. C. *J. Comp. Phys.* **1977**, *23*, 327-341). Energy minimization at the B3LYP/6-31G**/MM level was performed to compare with results from the QM(SCC-DFTB)/MM calculations (see Figure S1).

The umbrella sampling method[13] implemented in the CHARMM program along with the Weighted Histogram Analysis Method (WHAM)[14] was applied to determine the changes of the free energy (potential of mean force). The free energy curves for the wild-type enzyme (with and without the QM treatment of D164), D164N and T277A mutants were obtained as functions of ξ

= r(C-O$_\gamma$) for the inter-conversion between the tetrahedral adduct and aldehyde complexes. Harmonic biasing potentials were defined by the RESD module of CHARMM, with force constants in range of 100~800 kcal·mol^{-1}·Å^{-2}. The free energy curves for the nucleophilic attack and the reverse process were found to be similar (Figure S2). The QM region was enlarged to include W129 or T277 to examine the sensitivity of the free energy profiles on the inclusion of these two additional residues in the QM region. It was found that the results are similar (Figure S2). A further increase of the size of the QM region makes the free energy simulations very expensive, and such simulations were not performed. The systematic and statistical errors (Kobrak, M.N., J. Comput. Chem., 2003, 24, 1437) in the free energy calculations for the wild-type enzyme (i.e., the black solid line in Figure 3A) were determined, and the average error was estimated to be about ± 0.2 kca/mol.

Additional structural figures and 2-D free energy contour for the aldehyde complex

Figure Captions

Figure S1. Comparison of the average structure from the SCC-DFTB/MM MD simulations with the structure from B3LYP/6-31G** energy minimization (in parentheses). .

Figure S2. The D164N mutant. The average structures for the aldehyde (**A**) and hemiacetal complexes (**B**) based on the QM/MM free-energy simulations are given.

Figure S3. The T277A mutant. The average structures for the aldehyde (**A**) and hemiacetal complexes (**B**) based on the QM/MM free-energy simulations are given.
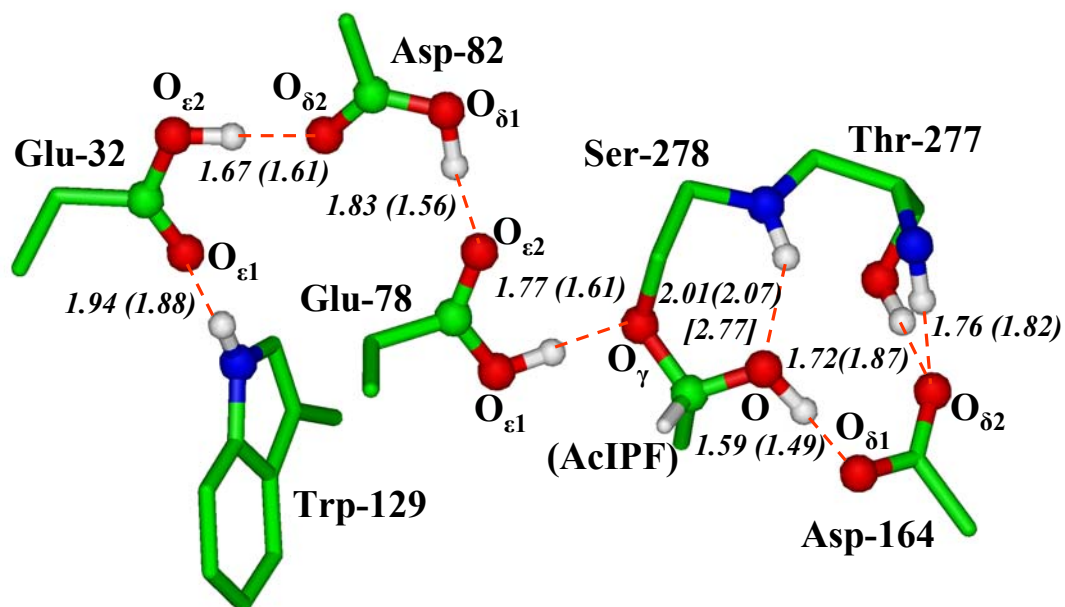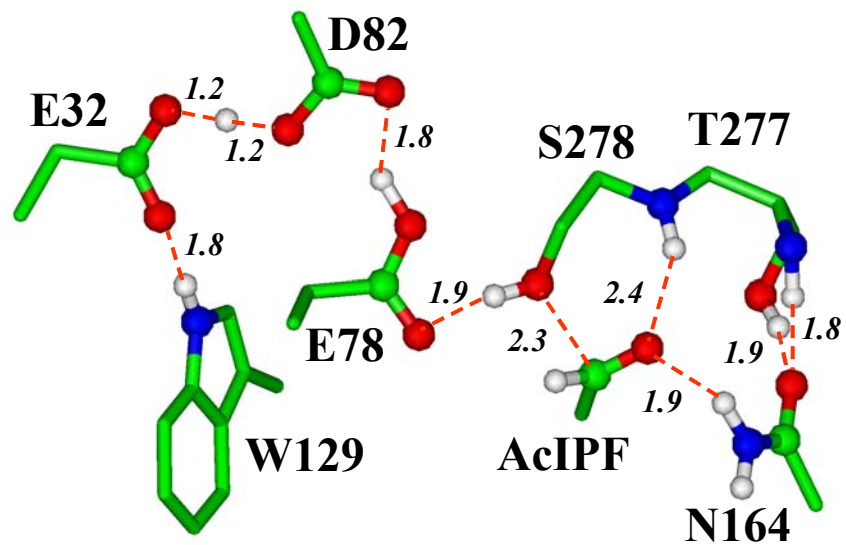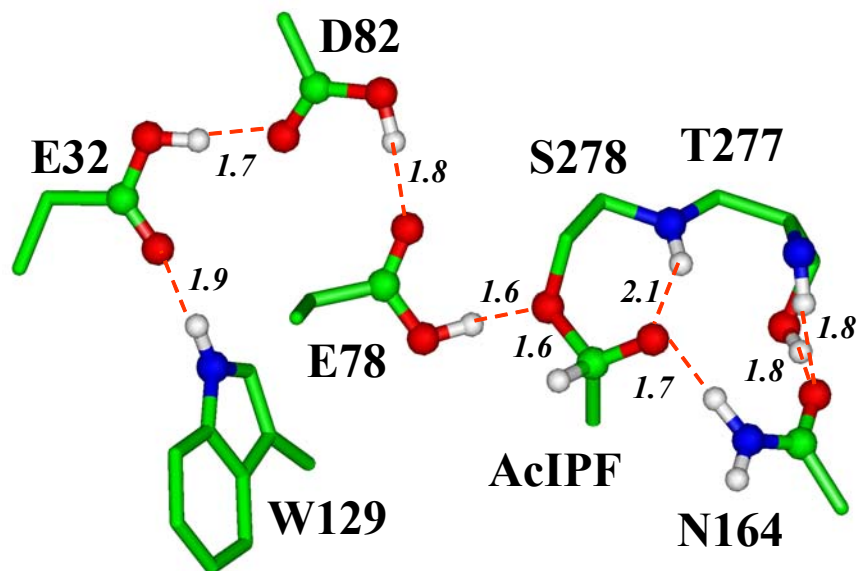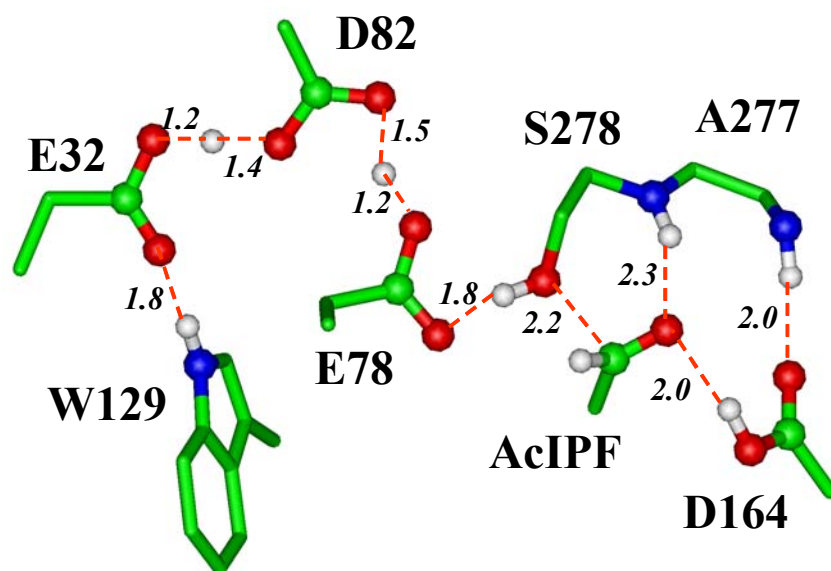
Figure S1

A

E32 · D82 · S278 · T277 · W129 · E78 · AcIPF · N164

B

D82 · E32 · S278 · T277 · E78 · W129 · AcIPF · N164

Figure S2

A

D82

E32

S278   A277

1.2   1.5
1.4   1.2

1.8

2.3

2.2   2.0

1.8

2.0

W129   E78   AcIPF   D164

B

D82

E32

S278   A277

1.7

1.8

1.8   2.0

1.8

1.9   1.6

W129   E78   AcIPF   D164
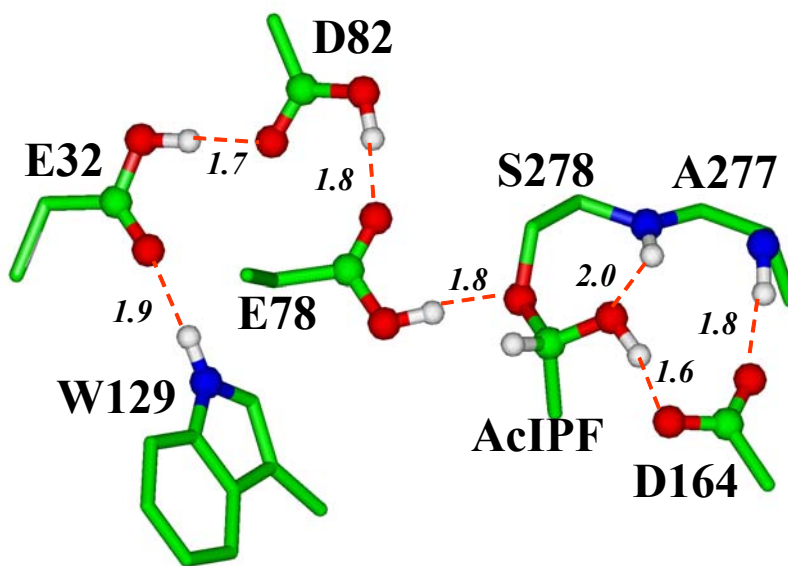
Figure S3

Complete Ref. 10

(10). Mackerell, A. D., Jr.; Bashford, D.; Bellott, M.; Bunbrack, R. L., Jr.; Evanseck, J. D.; Field, M. J.; Fischer, S.; Gao, J.; Guo, H.; Ha, S.; Joseph-McCarthy D.; Kuchnir, L.; Kuczera, K.; Lau, F. T. K.; Mattos, C.; Michnick, S.; Ngo, T.; Nguyen, D. T.; Prodhom, B.; Reiher, W. E. III; Roux, B.; Schlenkrich, M.; Smith, J. C.; Stote, R.; Straub, J.; Watanabe, M.; W.-Kuczera, J.; Yin, D.; Karplus, M. *J. Phys. Chem. B* **1998**, *102*, 3586-3616.